



Article

# Laser Textured Surfaces for Mixed Lubrication: Influence of Aspect Ratio, Textured Area and Dimple Arrangement

Johannes Schneider, Daniel Braun and Christian Greiner \*

Karlsruhe Institute of Technology (KIT), Institute for Applied Materials (IAM), Kaiserstrasse 12, 76131 Karlsruhe, Germany; johannes.schneider@kit.edu (J.S.); braun.daniel@me.com (D.B.)

\* Correspondence: greiner@kit.edu; Tel.: +49-721-608-41456

Received: 31 July 2017; Accepted: 9 August 2017; Published: 10 August 2017

**Abstract:** Unidirectional sliding experiments with polished and laser textured steel surfaces were carried out to investigate the effects of different textured area densities, aspect ratios and dimple arrangements. The system was lubricated with Polyalphaolefin (PAO) at 100 °C and the contact pressure was 3 MPa. For measuring Stribeck curves, the sliding speed was controlled between 40 and 2000 mm/s. The textured area density was varied between 5% and 30%, with the lowest friction values found for 10%. Aspect ratios ranging from 0.02 to 0.2 were investigated and for 0.1 the lowest friction values were measured. The dimple arrangements tested were cubic, hexagonal and a random distribution for a textured area density of 10% and an aspect ratio of 0.1. Our results demonstrate that the dimple arrangement does affect friction values, hinting to the fact that individual texture elements do influence each other. The optimum dimple arrangement was found in a hexagonal packing. This systematic variation of these three key texturing parameters for the morphological texturing of a tribological surface with dimples will allow a strategic choice of texturing parameters. This makes the most of the tremendous potential that laser surface texturing has for reducing friction forces and thereby CO<sub>2</sub> emissions.

**Keywords:** tribology; surface engineering; laser surface texturing; mixed lubrication; size effects

## 1. Introduction

Mankind needs to address alarming trends associated with global warming, such as rising sea levels that threaten vast coastal regions, declining crop production due to increased desertification and glacier melting that impacts water supplies [1]. Frictional energy losses have gained significant interest in the last years since the reduction of CO<sub>2</sub> emissions has become an important target of governments worldwide and as a major part of fossil fuels is used in transportation [2]. It is here where there is a great potential for reducing fuel consumption, and thereby CO<sub>2</sub> emissions, by minimizing frictional losses [3]. This in turn leads to an enormous need for new fuel saving technologies. One of these technologies is texturing the surface with micro dimples [4–6]. Such a surface texturing can be performed by indentation [7], chemical etching [8] or laser ablation [9]. Out of these techniques, laser surface texturing (LST) has prevailed as the most successful one due to its flexibility and ecological as well as economical superiority.

The field of regular micro textures dates back to the 1960s where Anno et al., introduced their theory about micro asperity lubrication [4,10,11]. In the 1990s, Etsion et al. [12,13] started working with regular micro dimples. In comparison to Anno et al., Etsion and coworkers used micro dimples or indents whereas Anno's asperities were protruding the surface. While dimples are more commonly used in order to decrease friction [14], channels and crossed channels are applied to increase friction, as might for example be desirable in clutch or break applications [15]. Regular

micro textures have proven beneficial under hydrodynamic and mixed lubrication conditions [14]. On the one hand, the underlying mechanisms in the hydrodynamic lubrication regime have been understood using numerical simulations [5]. On the other hand, the mechanisms for the textures' effectiveness under mixed lubrication are more complex due to the combination of solid-solid interaction and hydrodynamic lubrication. Generally speaking, simulations in the mixed lubrication regime are much more elaborate than in the hydrodynamic lubrication regime. Perhaps even more important for the practical applicability of a dimple-like morphological surface texture is the fact that also experimentally the influence of different texturing parameters, like the dimple packing density, spatial arrangement and aspect ratio on friction forces is not explicitly known due to a lack of systematic experiments. This is where our research comes in, aiming at establishing basic knowledge.

As far as current literature is concerned, systematic variations of the dimple diameter showed that there is an optimum in the dimple diameter [16–18] and that this optimum depends on the oil viscosity [18] and the velocity gradient along the contact area [17]. The aspect ratio [19] and the textured area [20] have been found to be as important as the lubricant viscosity, the sliding speed and the contact pressure.

In terms of texturing parameters and their influence on tribological properties, there is agreement in the literature that an optimum can be found around 0.1 [14,16,19,21,22], even though systematic experiments in which only the aspect ratio is varied and all other parameters are kept constant are missing. Additionally, numerical simulations in elasto-hydrodynamic lubrication indicated that the aspect ratio is the most important parameter with respect to building up additional hydrodynamic pressure [19,22]. Scaraggi et al., discussed reasons why there could be an optimum in the depth of micro dimples and so in the aspect ratio [23]. The authors are distinguishing two cases: with and without cavitation. In the absence of cavitation and by increasing the depth of the dimples (and so the aspect ratio), a transition in the fluid flow takes place to a different regime and vortex formation is leading to an increase in friction [23]. When cavitation takes place, the authors report that after an initially decreasing friction coefficient and as the dimples' depth increases (increasing aspect ratio), micro cavitation disappears and so the friction coefficient increases again [23].

A first research question that thus could be posed is whether the optimum at 0.1 is also effective under mixed lubrication, as there are publications finding the optimum at much smaller values around 0.01, especially for very low viscosity mediums like water [24,25]. For much higher viscosity gear oils, the optimum dimple aspect ratio was reported to be around 1.0 [26].

Another important parameter for enhancing tribological performance through a morphological surface texture is the textured area. Calculations by Brizmer et al., showed a linear increase in load capacity (the "load capacity" or "critical load" is the specific load where the system undergoes the transition from hydrodynamic to mixed lubrication) with increasing textured area [27]. Also, Peng et al. showed in their calculations that the frictional torque decreases with increasing textured area [25]. Experimental results on the other hand demonstrated in lubricated pin-on-disc tests that 5% to 20% textured area resulted in lower friction than 30% [28]. An optimum textured area was reported to be 5% in a lubricated system with dimples of 100–200  $\mu\text{m}$  in diameter and 5–10  $\mu\text{m}$  in depth [16]. In calculations for reciprocating automotive components, a variation of the textured area in a range between 5% and 20% influenced the friction force by only 7% [21]. In summary, there is not a consistent picture of how the textured area is affecting friction performance. In this contribution, we will therefore perform systematic experiments varying the textured area only (second research question).

A third parameter that beckons investigation is how the individual dimples are arranged on the surface (third research question). Closely associated is the issue whether the texturing elements are acting alone or if they are affecting each other, working as a collective. The hypothesis exists that in case the dimples are not influencing each other, the friction force is expected to decrease linearly with increasing textured area [25,27]. The aim of this contribution is to systematically analyze the influence of the depth to diameter ratio, the dimpled area and the packing pattern individually by in

each case keeping all other texturing parameters constant. For doing so, we measured Stribeck curves with a focus on the mixed lubrication regime for each tested set of texturing conditions.

## 2. Results

The steel pellets were successfully laser textured with the morphologies listed in Table 1, covering the systematic variation of aspect ratio, textured area and dimple arrangement. Based on data from previous studies [17,18], a texture with a dimple diameter of 40  $\mu\text{m}$ , a depth to diameter ratio of 0.1, a textured area of 10% and with a hexagonal dimple arrangement was chosen as the benchmark texture to compare the other surface morphologies to; in addition to the untextured, as-polished state that we also compare the performance of all surface morphologies to.

**Table 1.** Morphological surface textures generated by laser surface texturing. The benchmark texture, 40  $\mu\text{m}$  dimple diameter, aspect ratio 0.1, textured area 10% and hexagonal dimple arrangement, is listed in the second row. Deviations from this “standard” texture are highlighted in grey.

Diameter ( $w$ ) [ $\mu\text{m}$ ]	Depth ( $d$ ) [ $\mu\text{m}$ ]	Aspect Ratio ( $d/w$ )	Textured Area ( $a_{\text{tex}}$ ) [%]	Arrangement
40	2	0.05	10	Hexagonal
40	4	0.10	10	Hexagonal
40	8	0.20	10	Hexagonal
80	4	0.05	10	Hexagonal
200	4	0.02	10	Hexagonal
40	4	0.10	10	Random
40	4	0.10	10	Cubic
40	4	0.10	5	Hexagonal
40	4	0.10	20	Hexagonal
40	4	0.10	30	Hexagonal

In order to visualize the quality of our laser surface texturing and the differences in the morphologies tested, Figure 1 presents scanning electron and white light profilometry images of the three dimple arrangements.

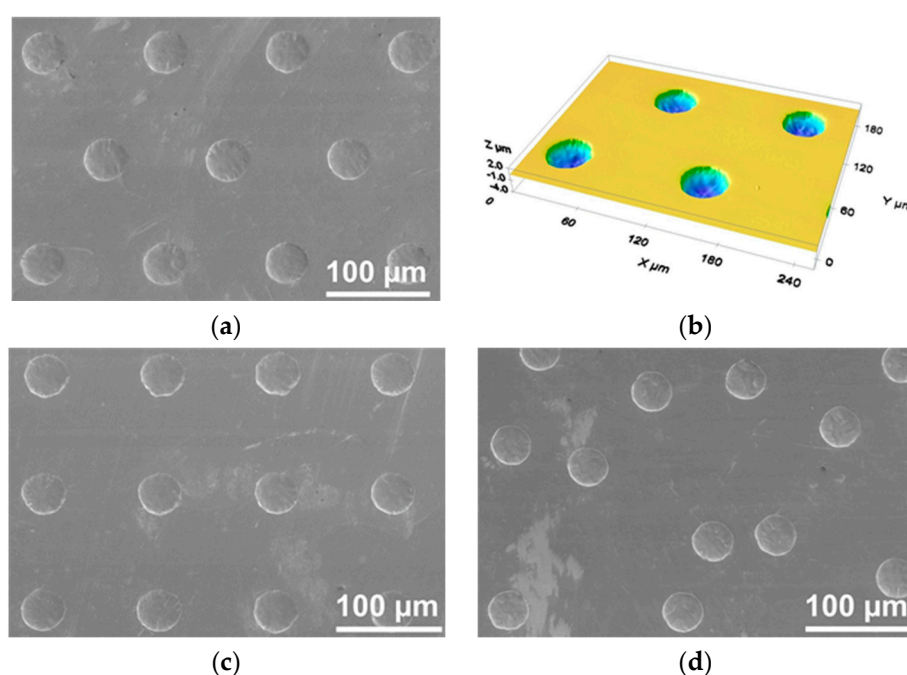


**Figure 1.** SEM and white light profilometry images of laser textured surfaces with different dimple arrangements. Textured steel (C85) samples with circular dimples of 40  $\mu\text{m}$  in diameter, a depth of 4  $\mu\text{m}$  and a packing density of 10%. (a,b) hexagonal, (c) cubic, and (d) random arrangement.

The texturing elements (circular dimples) had a diameter of 40 to 200  $\mu\text{m}$ , an aspect ratio between 0.05 and 0.2 and covered 5% to 30% of the pellet surface. They were arranged in a hexagonal (Figure 1a,b), cubic (Figure 1c), or random (Figure 1d) fashion.

### 2.1. Influence of the Aspect Ratio

The following experiments were carried out under a contact pressure of 3 MPa (150 N normal force) and at a temperature of 100  $^{\circ}\text{C}$ . The lubrication was Polyalphaolefin (PAO) with a viscosity of 4  $\text{mm}^2/\text{s}$ .

In order to systematically vary the aspect ratio, the textured area was kept constant at 10% and a hexagonal dimple arrangement was chosen. In Figure 2, the friction coefficient of samples having been textured with dimples whose aspect ratio is ranging from 0.05 to 0.2 are compared to the friction performance of the polished reference.

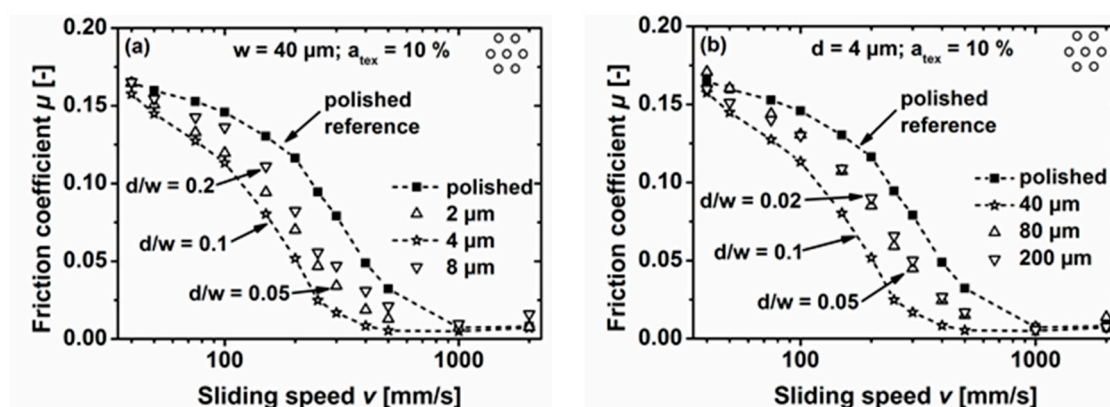


**Figure 2.** Variation of the dimple aspect ratio. Friction coefficient plotted against the sliding speed for the polished reference and surfaces textured with dimples having aspect ratios ranging from 0.05 to 0.2. (a) Variation of the aspect ratio by keeping the dimple diameter (40  $\mu\text{m}$ ) and textured area (10%) as well as the dimple arrangement (hexagonal) constant. The sliding speed is plotted in a logarithmic fashion in order to ease the comparison in the mixed lubrication regime; (b) Variation of the aspect ratio by keeping the dimple depth constant (4  $\mu\text{m}$ ) and systematically changing the dimple diameter between 40 and 200  $\mu\text{m}$ . All other parameters were kept the same as in (a).

Our first approach to systematically vary the aspect ratio was based on keeping the dimple diameter constant at 40  $\mu\text{m}$  and changing the dimple depth between 2 to 8  $\mu\text{m}$  (Figure 2a). The data shows that all morphological surface textures lead to a reduction in friction coefficient compared to the polished reference. Among these textures, the dimples with an aspect ratio of 0.1 resulted in the smallest friction coefficients (82% friction reduction compared to the polished reference; at a sliding speed of 0.4 m/s). Aspect ratios higher (0.2) or lower (0.05) than 0.1 resulted in friction forces between the polished reference and the dimples with an aspect ratio of 0.1; with an aspect ratio of 0.05 slightly beneficial to 0.2 (61% friction reduction).

Another approach to changing the aspect ratio systematically is by keeping the dimple depth constant, in our case at 4  $\mu\text{m}$ , and varying the dimple diameter. The results of these experiments are shown in Figure 2b where the diameter was varied between 40 and 200  $\mu\text{m}$ . As in the case when the dimple depth was systematically altered (Figure 2a), also here, the surface texture with dimples having an aspect ratio of 0.1 resulted in the highest reduction in friction coefficient (82%, same texture as above), compared to the polished reference. The difference between aspect ratios of 0.02 and 0.05 with 8% is rather small over the complete range of tested sliding speeds. Interestingly, the sample with very low aspect ratios (0.05) is the only one that leads to an increase in friction compared to the polished reference (for a sliding speed of 40 mm/s).

## 2.2. Influence of the Textured Area

As the next parameter of interest, the textured area was varied between 5% and 30% and the friction performance of the respective samples compared to that of the polished reference. The dimple diameter and the dimple depth were both kept constant at 40 and 4  $\mu\text{m}$  respectively (aspect ratio of 0.1); the dimples were arranged hexagonally on the surface. The resulting friction data are presented in Figure 3.

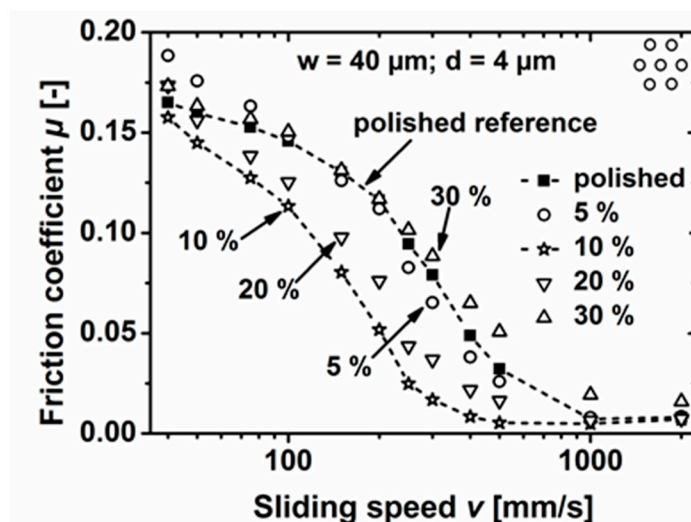


**Figure 3.** Variation of the dimple packing density. Friction coefficient plotted against the sliding speed for the polished reference and surfaces with dimple packing densities between 5% and 30%. The dimple diameter was kept constant at 40  $\mu\text{m}$ , the depth at 4  $\mu\text{m}$  (aspect ratio of 0.1) and all dimples were arranged in a hexagonal pattern. The sliding speed is plotted in a logarithmic fashion in order to ease the comparison in the mixed lubrication regime.

When comparing these different textured area densities, it becomes apparent that covering 10% of the contact area with dimples resulted in the highest friction reduction (82%) compared to the polished reference. In the case of the 5% textured area, there is nearly no (sliding speed above 100 mm/s) or a negative ( $\leq 100$  mm/s) effect of the textures. Increasing the textured area density to 20% or 30% leads to an increase in friction compared to the surface with 10% textured area. In case of a packing density of 20%, the friction coefficient is however still below that of the polished reference. For a packing density of 30%, this changes and the friction performance is slightly above that of the polished sample for nearly every sliding speed. Only in the region between 150 and 200 mm/s, we measured roughly the same friction coefficient as for the polished reference.

## 2.3. Influence of the Dimple Arrangement

The third and final parameter to be systematically studied is the nature of the dimple arrangement on the surface. For these experiments, the textured area was kept constant at 10%, the dimple diameter at 40  $\mu\text{m}$  and the dimple depth at 4  $\mu\text{m}$  (aspect ratio of 0.1). A hexagonal and a cubic arrangement of the dimples on the surface were compared to a structure where the dimples were distributed in a random fashion. Figure 4 presents the results from these experiments.

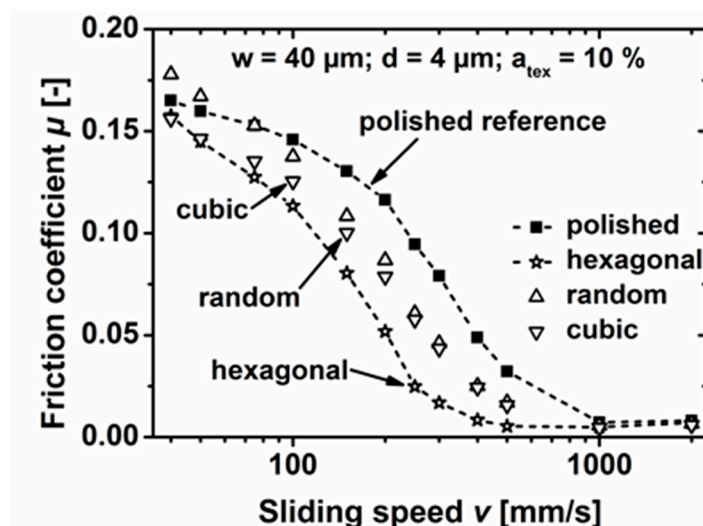


**Figure 4.** Variation of the dimple arrangement on the surface. Friction coefficient plotted against the sliding speed for the polished reference and surfaces with dimples arranged in a hexagonal, cubic and random fashion. The dimple diameter was kept constant at  $40 \mu\text{m}$ , the depth at  $4 \mu\text{m}$  (aspect ratio of 0.1) and the packing density was 10%. The sliding speed is plotted in a logarithmic fashion in order to ease the comparison in the mixed lubrication regime.

Figure 4 demonstrates that among the dimple arrangements tested, the hexagonal one resulted in the largest reduction in friction coefficient (82%) compared to the polished reference. The randomly distributed and cubically arranged dimples show friction forces in between the polished reference and hexagonal dimple arrangement. They do reduce friction forces (50% for cubic and 48% for random), but by far not as pronounced as a hexagonal alignment. At very low sliding speeds ( $<50 \text{ mm/s}$ ) the randomly distributed dimples were increasing the friction compared to the polished reference. At medium sliding speeds (200 to 500 mm/s) there is virtually no difference between the cubic and randomly arranged dimples.

### 3. Discussion

The tribological properties of laser textured steel samples were characterized in order to systematically investigate the influence of the dimple aspect ratio, packing density and arrangement. These experiments were carried out in lubricated (PAO-18,  $100 \text{ }^\circ\text{C}$ ) unidirectional contact with 3 MPa nominal contact pressure. The sliding speed was varied between 40 and 2000 mm/s in order to achieve Stribeck curves, while concentrating on the mixed lubrication regime.

The aspect ratio was varied between 0.05 and 0.2. The reason why we concentrated on aspect ratios around 0.1 is that other authors previously reported an optimal aspect ratio for values of approximately 0.1 [19,26,29–32]. There was one notable exception, where an optimum at 0.01 was found [24]. It should be noted, however, that in most of these publications several texturing parameters were varied simultaneously, sometimes making it difficult to precisely assess the influence of each individual parameter. Assuming that the dimples' packing density and their arrangement on the surface are both kept constant, there are two ways to systematically change the aspect ratio. One is by varying the dimple depth, while keeping the dimple diameter the same; the other is by holding the dimple depth constant while systematically changing the dimple diameter. We chose both routes in order to systematically investigate whether these two approaches yield different answers to the question for the optimum dimple aspect ratio. As can be seen in Figure 2a and 2b, the approach does not significantly change the results and the answer in both cases is that the optimum lies at 0.1, which is in agreement with the majority of the existing literature.

This optimum is also substantiated by numerical simulations [19,22] that were carried out for the elastohydrodynamic lubrication regime. Interestingly, there is no constant decrease or increase in friction when changing the aspect ratio. This might hint to the fact that there are two competing

mechanisms at play, yielding an optimum at 0.1. One of these mechanisms might be found in the additional micro-hydrodynamic pressure built-up through a dimple-like morphological surface texture [17,28]. Once the dimples are too shallow, the flow necessary to build-up this additional lift can no longer be established. This effect is not only affected by the dimple diameter, as described in a previous publication [18], but also by the dimple depth. Following this train of thought, deeper dimples (like the ones with an aspect ratio of 0.2 and 8  $\mu\text{m}$  depth) are expected to build up at least as much pressure as the ones with an aspect ratio of 0.1. This is not the case (see Figure 2a). The reason for this behavior might be found in the possible second, competing, mechanism. It was already speculated in the literature that the formation of a vortex inside the dimple, or cavitation are only possible within a certain range of aspect ratios. The dependence of such phenomena on dimple depth therefore is an interesting question to follow with future research. Employing a unidirectional in situ tribometer, we had in the past already studied cavitation phenomena for a morphological surface texture consisting of crossed micro-channels [33].

The other mechanisms, besides a micro-hydrodynamic pressure build-up and cavitation, postulated in the literature, possibly responsible for reducing friction and wear by a morphological surface texture, are a change in contact angle due to the altered surface morphology [34], the trapping of wear particles [35] and the possible storage of lubricant inside the dimples [36]. None of these mechanisms are expected to be decisively impacted by a variation in aspect ratio, permitting to focus the discussion on fluid dynamic effects.

The second texturing parameter that was systematically varied was the textured area (Figure 3). Our data shows a clear minimum in friction coefficient for a textured area of 10%. As the range of textured areas was between 5% and 30%, this—like in the case of the aspect ratio—means that there is no clear trend for the friction force as a function of the textured area. Rather, we again find an optimal value. In the existing literature, one can find authors who concluded that the textured area has very little influence [31], while others reported that a textured area of 5% yielded the lowest friction forces experimentally and of 40% in the corresponding numerical study [24]. Here, as in our case, friction forces were lowered by about 75% through introducing a texture with a packing density of 10% [24]. Since in our data (Figure 3), friction forces even increased for the 30% surface texture, we can unequivocally state that the textured area is an important parameter having a decisive impact on the success of laser surface texturing. The contrast to some of the existing literature, e.g., [37], might be explained through the fact that in our study, in contrast to most of the existing literature, the textured area was the only parameter systematically varied.

For pure hydrodynamic sliding, calculations predicted a linear increase in the load bearing capacity (for dimple aspect ratios comparable to ours) with the textured area [25,27]. As such a trend is clearly not seen in our data, other mechanisms seem to be dominating in mixed compared to hydrodynamic lubrication.

As to what these mechanisms are, we can only speculate. The proposed mechanism of lubricant storage inside the dimples clearly fails to explain our data, as friction forces increase for the 30% surface texture for small sliding speeds. A better explanation might be found in the fact that with increasing textured area, the real contact area decreases. In an unlubricated solid–solid contact with laser textured samples, we could previously show that the laser texturing parameters have a significant influence on static friction forces [38]. As in mixed lubrication solid–solid contacts play a decisive role, a similar effect on dynamic friction could be hypothesized. At the very least, it is absolutely feasible that as the real contact pressure increases with the textured area, there will be an influence on the tribological behavior of the contact. At the same time, such a trend would be expected to be continuous with the textured area and does not explain the optimum found here. When thinking about a second, competing mechanism, a possible candidate is found in the question of whether each dimple is acting on its own (the macroscopic behavior basically being the sum of its constituents) or if they are acting as a collective (the macroscopic behavior not being the sum of its constituents).

A first approach to answering this question can be taken by comparing the samples with 5 and 10% textured area. In the case where there were no interactions between the dimples, one would

expect the amount of friction reduction to scale linearly with the textured area. The reason for this expected linear behavior is that in the case of 5% textured area, there are about 2000 dimples on the 8 mm diameter pellet (area: 50 mm<sup>2</sup>) surface. In the case of the 10% textured area, there are twice as many dimples in the contact (4000 dimples). Now comparing different measured friction coefficients, e.g., at a constant sliding speed of 400 mm/s, one finds that for 5% textured area the friction coefficient is 0.038, whereas for 10% it is 0.008. Comparing these numbers to the polished reference ( $\mu = 0.049$ ), introducing 5% of textured area decreased the friction coefficient by 22%, while a 10% textured area lowered  $\mu$  by 83%. Therefore, there clearly is no linear correlation between the friction coefficient and the textured area. This is a strong indication that the dimples do not act individually, but rather as a collective.

To further investigate this extremely important question, we performed experiments with different dimple packing patterns, the hypothesis being that in case the dimples act individually, the packing pattern is not expected to change the tribological behavior. As can be clearly seen in Figure 4, this is not the case, again leading to the conclusion that the dimples operate as a collective. These results are also in agreement with literature. When solving the Reynolds equation for evaluating the hydrodynamic pressure created by dimples of different alignment, Wang et al. calculated varying hydrodynamic pressures for different angles between rows of dimples (and thereby distance between the individual dimples) [39]. Yu et al., solved the Reynolds equation for nine dimples arranged in a square pattern [40]. Their results demonstrate an overlap between the pressure distributions created by each individual dimple.

The data presented above highlights the enormous potential of creating a morphological surface texturing by means of laser radiation for reducing friction forces. With a strategically chosen combination of texturing parameters, mainly the dimple diameter, aspect ratio, packing density and dimple arrangement, friction reductions by over 80% can be achieved. Unlike with our previous results for the optimal dimple diameter, which strongly depended on system parameters [18], the optimum values for aspect ratio, packing density and arrangement are expected to be significantly more stable when changing the conditions of the tribological system. This expectation is strengthened by our own previous results for surface textured ceramic-steel contacts [41]. As this study was performed with isoctane instead of PAO, elucidating how lubricants with different viscosities and molecular weights [42] influence the optimum texturing parameters is part of our ongoing research efforts. A laser texturing parameter that will be systematically studied in the future is the cross-sectional profile of the dimples. Numerical results already indicated a significant influence of this texturing degree of freedom [43]. Also, experimentally there are first indications that the dimple profile is an important texturing parameter [44].

While our research discussed here focused mainly on friction, the question how these morphological surface textures influence wear is left open. Due to the small friction forces made possible through laser surface texturing and with our current experimental capabilities for measuring wear—based on white light interferometry—there was no discernible wear after the experiments. Investigating wear in more detail will therefore involve performing experiments either over much longer sliding distances or under more severe wear conditions, e.g., higher contact pressures. Moreover, this is interesting as laser textured surfaces are sometimes covered with hard coatings like diamond like carbon (DLC), especially when trying to protect the surface against wear and corrosion [45]. Comparing the performance of an optimal morphological surface texture with and without a hard coating in terms of wear performance will therefore be of future interest.

## 4. Materials and Methods

### 4.1. Sample Material

A pin-on-disc configuration was used to characterize the tribological properties of laser textured as well as polished steel pins sliding against steel discs. The 8 mm pins were made out of C85 steel (Stahlbecker, Heusenstamm, Germany). C85 with a hardness of 400 HV and in a normalized state was chosen due of its very fine and homogeneous pearlitic grain structure. The

pins were first ground (200 mesh) and then polished using 3 and 1  $\mu\text{m}$  diamond suspensions (Cloeren Technology, Wegberg, Germany), down to a final roughness  $R_a$  of around 4 nm.

The 70 mm diameter discs were made out of 100Cr6 (AISI 5210, Eisen Schmidt, Karlsruhe, Germany) in a hardened and tempered (190 °C) state (approx. 800 HV). These discs were grinded (200 mesh) to a roughness ranging from  $R_a = 0.08$  to  $0.12 \mu\text{m}$ . The surface quality was monitored by a tactile roughness measurement device (Hommel T8000, Jenoptic, Jena, Germany) and a white light profilometer (Sensofar Plu neox, Sensofar, Barcelona, Spain). The waviness (2nd order according to DIN 4760) of the discs had to be less than 1  $\mu\text{m}$  along the frictional radius of 30 mm.

#### 4.2. Laser Surface Texturing

The laser surface texturing (LST) was performed with the a pulsed (100 ns) Yb-doped fiber laser. The Piranha II system from Acsys (Kornwestheim, Germany) used a laser source (YLP-1-100-20-20) from IPG Photonics (Oxford, MA, USA) with 1064 nm wavelength. As in a previous publication [18], the influence of the dimple diameter on the tribological performance of morphologically textured surfaces was investigated in detail, we here decided to test the influence of aspect ratio, packing density and packing pattern with three distinct dimple diameters. These were 40, 80 and 200  $\mu\text{m}$ . The 40  $\mu\text{m}$  diameter textures were created with single pulses. By moving the laser beam in a defined velocity over the surface, the distance between the dimples could be varied. By controlling the distance between two individual dimples and additionally between the lines of the dimples, the arrangement and the textured area was defined. Increasing the number of laser pulses for each individual dimple, controlled the dimple's depth. To generate a truly random dimple pattern on the surface, we made use of the randomizer built into the computing environment Maple (version 11, Maplesoft, Waterloo, ON, Canada). We generated a random distribution of points and had the laser beam directly approach these points, creating each dimple, one by one.

There are two ways to vary the aspect ratio systematically, one by changing the dimple depth as described above and the other by varying the dimple diameter at constant dimple depth. Therefore, dimples with 80 and 200  $\mu\text{m}$  were created with 4  $\mu\text{m}$  dimple depth. For these dimples, Archimedes spirals were used as described in [46]. All the dimples created in this study had the cross-sectional contour of a hemispherical indent and a self-similar shape.

Since a nanosecond laser was used to create these texture elements, after the laser process, debris had formed around the dimples. This debris had to be removed by an additional polishing step prior to all tribological tests. Polishing was performed by making use of 3 and 1  $\mu\text{m}$  diamond suspensions. Right before tribological testing, all samples were cleaned by ultrasound in Acetone (grade: pure) and Isopropanol (grade: for synthesis) for five minutes each. Strict quality management of all sample preparation steps, including the laser surface texturing, was performed by closely monitoring each sample by optical, digital and 3D microscopy, images being taken before and after each processing step; and before and after the tribological testing.

#### 4.3. Tribological Testing

A pin-on-disc tribometer (Plint TE-92 HS, Phoenix Tribology, Kingsclere, UK) was used to carry out the tribological characterization of the different morphological surface textures, as well as of the polished reference. The normal force in all experiments was 150 N, corresponding to a nominal contact pressure of 3 MPa. The sliding speed was varied between 40 and 2000 mm/s in order to investigate different friction regimes (mainly mixed and hydrodynamic lubrication) following Stribeck [47], who described the dependency of frictional forces on the sliding speed, normal load and lubricant viscosity. Even if we were mainly interested in the performance of our samples in the mixed lubrication regime, we found it to be of interest to choose Stribeck parameters ranging from the mixed to the hydrodynamic lubrication regime, as this allowed us to determine where the transition between these two regimes takes place. The mean frictional radius, i.e., the distance between the center of the pellet and the center of the disc, was 30 mm. All experiments were carried out at 100 °C system temperature. This was achieved by heating not only the oil itself, but also the testing cell including the pellet and its holder, as well as the disc. This approach led to a very

uniform and stable system temperature with a deviation below 1 K. The test setup was lubricated with poly-alpha-olefin (PAO) from Klüber Lubrication (Munich, Germany). Its viscosity was 4 mm<sup>2</sup>/s at 100 °C; the oil flow rate was 125 mL/h.

The tribological tests were started at a sliding speed of 2000 mm/s, which was then followed by a stepwise decrease down to the lowest speed of 40 mm/s, holding each individual step for 300 s. This protocol generated Stribeck curves, following [30]. These speed ramps were repeated five times for each sample and out of the last three ramps a mean value was calculated in order to avoid any possible running-in influences. Each texture was tested at least twice with a completely new pin and disc pair. Further details about the tribological tests can be found in the supporting information section of a previous paper [18].

## 5. Conclusions

Steel surfaces were laser surface textured by means of an Yb-doped fiber laser with spherical dimples. In order to methodically investigate the influence of different texturing parameters, the dimples' aspect ratio was systematically varied between 0.02 and 0.2 by either changing the dimple depth and simultaneously keeping the dimple diameter constant, or by changing the dimple diameter at constant dimple depth. Second, the packing density of the dimples on the textured surface was varied between 5% and 30%. Third, we tested a hexagonal, cubic and random dimple packing pattern. The textured pins, made out of C85 steel, were then paired against bearing steel 100Cr6 discs in unidirectional pin-on-disc experiments, lubricated with PAO. The contact pressure was kept constant at 3 MPa, the system temperature was 100 °C and sliding speeds varied between 40 to 2000 mm/s, in order to independently investigate the effect of these three texturing parameters in the mixed lubrication regime. Ultimately, we wanted to answer the question which combination of texturing parameters yields the smallest friction forces. The main results of these experiments can be summarized as follows:

- Friction reduction is the highest for a dimple aspect ratio of 0.1, regardless whether one changes the aspect ratio by varying the dimple diameter or the dimple depth.
- A dimple packing density of 10% leads to the maximum reduction in friction forces.
- The dimples do not act individually, but as a collective. Arranging them in a hexagonal pattern is superior to a cubic, or random layout.
- The samples did not exhibit any significant amount of wear.
- A maximum friction reduction of over 80% was realized, demonstrating the tremendous potential of laser surface texturing for reducing friction and increasing energy efficiency.

**Acknowledgments:** The authors acknowledge financial support by Daimler AG, Robert Bosch GmbH, KSPG Automotive and Klüber Lubrication München KG. Thanks are due to Paul Schreiber and Karsten Wolff for laser texturing. Christian Greiner acknowledges funding by the German Research Foundation DFG under Project GR 4174/1.

**Author Contributions:** Johannes Schneider and Christian Greiner conceived and designed the experiments; Daniel Braun performed the experiments; Christian Greiner, Johannes Schneider and Daniel Braun analyzed the data; Daniel Braun and Christian Greiner wrote the paper.

**Conflicts of Interest:** The authors declare no conflict of interest.

## References

1. Olivier, J.G.J.; Janses-Maenhout, G. *CO<sub>2</sub> Emissions from Fossil Fuel Combustion Part III: Total Green House Gas Emissions*; International Energy Agency: Paris, France, 2015.
2. Holmberg, K.; Andersson, P.; Erdemir, A. Global energy consumption due to friction in passenger cars. *Tribol. Int.* **2012**, *47*, 221–234.
3. Carpick, R.W.; Jackson, A.; Sawyer, W.G.; Argibay, N.; Lee, P.; Pachon, A.; Gresham, R.M. Can tribology save a quad. *Tribol. Lubr. Technol.* **2016**, *72*, 44–45.
4. Etsion, I. *State of the Art in Laser Surface Texturing*; Tsinghua University Press: Beijing, China, 2009; pp. 761–762.

5. Gropper, D.; Wang, L.; Harvey, T.J. Hydrodynamic lubrication of textured surfaces: A review of modeling techniques and key findings. *Tribol. Int.* **2016**, *94*, 509–529.
6. Ibatan, T.; Uddin, M.; Chowdhury, M. Recent development on surface texturing in enhancing tribological performance of bearing sliders. *Surf. Coat. Technol.* **2015**, *272*, 102–120.
7. Pettersson, U.; Jacobson, S. Tribological texturing of steel surfaces with a novel diamond embossing tool technique. *Tribol. Int.* **2006**, *39*, 695–700.
8. Costa, H.L.; Hutchings, I.M. Development of a maskless electrochemical texturing method. *J. Mater. Process. Technol.* **2009**, *209*, 3869–3878.
9. Vilhena, L.M.; Sedlaček, M.; Podgornik, B.; Vižintin, J.; Babnik, A.; Možina, J. Surface texturing by pulsed Nd:YAG laser. *Tribol. Int.* **2009**, *42*, 1496–1504.
10. Anno, J.N.; Walowit, J.A.; Allen, C.M. Microasperity lubrication. *J. Lubr. Technol.* **1968**, *90*, 351–355.
11. Gachot, C.; Rosenkranz, A.; Hsu, S.M.; Costa, H.L. A critical assessment of surface texturing for friction and wear improvement. *Wear* **2017**, *372*, 21–41.
12. Etsion, I.; Burstein, L. A model for mechanical seals with regular microsurface structure. *Tribol. Trans.* **1996**, *39*, 677–683.
13. Etsion, I.; Kligerman, Y.; Halperin, G. Analytical and experimental investigation of laser-textured mechanical seal faces. *Tribol. Trans.* **1999**, *42*, 511–516.
14. Kligerman, Y.; Etsion, I.; Shinkarenko, A. Improving tribological performance of piston rings by partial surface texturing. *J. Tribol.* **2005**, *127*, 632–638.
15. Zum Gahr, K.H.; Wahl, R.; Wauthier, K. Experimental study of the effect of microtexturing on oil lubricated ceramic/steel friction pairs. *Wear* **2009**, *267*, 1241–1251.
16. Yan, D.; Qu, N.; Li, H.; Wang, X. Significance of dimple parameters on the friction of sliding surfaces investigated by orthogonal experiments. *Tribol. Trans.* **2010**, *53*, 703–712.
17. Greiner, C.; Merz, T.; Braun, D.; Codrignani, A.; Magagnato, F. Optimum dimple diameter for friction reduction with laser surface texturing: The effect of velocity gradient. *Surf. Topogr. Metrol. Prop.* **2015**, *3*, 044001.
18. Braun, D.; Greiner, C.; Schneider, J.; Gumbsch, P. Efficiency of laser surface texturing in the reduction of friction under mixed lubrication. *Tribol. Int.* **2014**, *77*, 142–147.
19. Shinkarenko, A.; Kligerman, Y.; Etsion, I. The validity of linear elasticity in analyzing surface texturing effect for elasto-hydrodynamic lubrication. *J. Tribol.* **2009**, *131*, 021503.
20. Wang, X.L.; Kato, K.; Adachi, K.; Aizawa, K. The effect of laser texturing of sic surface on the critical load for transition of water lubrication mode from hydrodynamic to mixed. *Tribol. Int.* **2001**, *34*, 703–711.
21. Ronen, A.; Etsion, I.; Kligerman, Y. Friction-reducing surface-texturing in reciprocating automotive components. *Tribol. Trans.* **2001**, *44*, 359–366.
22. Shinkarenko, A.; Kligerman, Y.; Etsion, I. The effect of elastomer surface texturing in soft elasto-hydrodynamic lubrication. *Tribol. Lett.* **2009**, *36*, 95–103.
23. Scaraggi, M.; Mezzapesa, F.P.; Carbone, G.; Ancona, A.; Sorgente, D.; Lugarà, P.M. Minimize friction of lubricated laser-microtextured-surfaces by tuning microholes depth. *Tribol. Int.* **2014**, *75*, 123–127.
24. Wang, X.; Kato, K.; Adachi, K.; Aizawa, K. Loads carrying capacity map for the surface texture design of sic thrust bearing sliding in water. *Tribol. Int.* **2003**, *36*, 189–197.
25. Peng, X.D.; Sheng, S.E.; Li, J.Y.; Pan, X.M.; Bai, S.X. Effects of dimple geometric parameters on the performance of a laser-textured mechanical seal. *Key Eng. Mater.* **2008**, *373–374*, 766–769.
26. Ramesh, A.; Akram, W.; Mishra, S.P.; Cannon, A.H.; Polycarpou, A.A.; King, W.P. Friction characteristics of microtextured surfaces under mixed and hydrodynamic lubrication. *Tribol. Int.* **2013**, *57*, 170–176.
27. Brizmer, V.; Kligerman, Y.; Etsion, I. A laser surface textured parallel thrust bearing. *Tribol. Trans.* **2003**, *46*, 397–403.
28. Wakuda, M. Effect of surface texturing on friction reduction between ceramic and steel materials under lubricated sliding contact. *Wear* **2003**, *254*, 356–363.
29. Chae, Y.H. In Effect of size for micro-scale dimples on surface under lubricated sliding contact. *Key Eng. Mater.* **2007**, *345*, 765–768.
30. Shinkarenko, A.; Kligerman, Y.; Etsion, I. The effect of surface texturing in soft elasto-hydrodynamic lubrication. *Tribol. Int.* **2009**, *42*, 284–292.
31. Kim, B.; Chae, Y.H.; Choi, H.S. Effects of surface texturing on the frictional behavior of cast iron surfaces. *Tribol. Int.* **2014**, *70*, 128–135.

32. Shinkarenko, A.; Kligerman, Y.; Etsion, I. Theoretical analysis of surface-textured elastomer sleeve in lubricated rotary sliding. *Tribol. Trans.* **2010**, *53*, 376–385.
33. Wahl, R.; Schneider, J.; Gumbusch, P. In situ observation of cavitation in crossed microchannels. *Tribol. Int.* **2012**, *55*, 81–86.
34. Ma, C.H.; Bai, S.X.; Peng, X.D.; Meng, Y.G. Improving hydrophobicity of laser textured sic surface with micro-square convexes. *Appl. Surf. Sci.* **2013**, *266*, 51–56.
35. Varenberg, M.; Halperin, G.; Etsion, I. Different aspects of the role of wear debris in fretting wear. *Wear* **2002**, *252*, 902–910.
36. Lu, X.; Khonsari, M. An experimental investigation of dimple effect on the stribeck curve of journal bearings. *Tribol. Lett.* **2007**, *27*, 169.
37. Kovalchenko, A.; Ajayi, O.; Erdemir, A.; Fenske, G.; Etsion, I. The effect of laser texturing of steel surfaces and speed-load parameters on the transition of lubrication regime from boundary to hydrodynamic. *Tribol. Trans.* **2004**, *47*, 299–307.
38. Greiner, C.; Schaefer, M.; Popp, U.; Gumbusch, P. Contact splitting and the effect of dimple depth on static friction of textured surfaces. *ACS Appl. Mater. Interface* **2014**, *6*, 7986–7990.
39. Yu, H.; Huang, W.; Wang, X. Dimple patterns design for different circumstances. *Lubr. Sci.* **2013**, *25*, 67–78.
40. Yu, H.; Deng, H.; Huang, W.; Wang, X. The effect of dimple shapes on friction of parallel surfaces. *Proc. Inst. Mech. Eng. Part J: J. Eng. Tribol.* **2011**, *225*, 693–703.
41. Wöppermann, M.; Zum Gahr, K.H. Surface textured steel/ceramic and ceramic/ceramic pairs sliding in isooctane. In *Friction, Wear and Wear Protection*; Wiley-VCH: Weinheim, Germany, 2009; pp. 362–368.
42. Karuppiyah, K.K.; Sundararajan, S.; Xu, Z.-H.; Li, X. The effect of protein adsorption on the friction behavior of ultra-high molecular weight polyethylene. *Tribol. Lett.* **2006**, *22*, 181–188.
43. Knoll, G. Elastohydrodynamic simulation technology with integrated mixed lubrication. *Materialwissenschaft und Werkstofftechnik* **2003**, *34*, 946–952.
44. Lu, P.; Wood, R.J.K.; Gee, M.G.; Wang, L.; Pfleging, W. The use of anisotropic texturing for control of directional friction. *Tribol. Int.* **2017**, *113*, 169–181.
45. Li, X.; Bhushan, B. Micromechanical and tribological characterization of hard amorphous carbon coatings as thin as 5 nm for magnetic recording heads. *Wear* **1998**, *220*, 51–58.
46. Gao, Y.; Wu, B.; Zhou, Y.; Tao, S. A two-step nanosecond laser surface texturing process with smooth surface finish. *Appl. Surf. Sci.* **2011**, *257*, 9960–9967.
47. Stribeck, R. Die wesentlichen Eigenschaften der Gleit- und Rollenlager. *Z. Verein. Deut. Ing.* **1902**, *46*, 1341–1348 (pt I), 1432–1438 (pt II), 1463–1470 (pt III).



© 2017 by the authors. Licensee MDPI, Basel, Switzerland. This article is an open access article distributed under the terms and conditions of the Creative Commons Attribution (CC BY) license (<http://creativecommons.org/licenses/by/4.0/>).